THE JOURNAL OF BIOLOGICAL CHEMISTRY
Vol. 276, No. 19, Issue of May 11, pp. 16302–16309, 2001
Printed in U.S.A.
© 2001 by The American Society for Biochemistry and Molecular Biology, Inc.

Factor IXa:Factor VIIIa Interaction

HELIX 330–338 OF FACTOR IXa INTERACTS WITH RESIDUES 558–565 AND SPATIALLY ADJACENT REGIONS OF THE A2 SUBUNIT OF FACTOR VIIIa*

Received for publication, December 26, 2000
Published, JBC Papers in Press, February 14, 2001, DOI 10.1074/jbc.M011680200

S. Paul Bajaj‡§, Amy E. Schmidt‡, Akash Mathur‡, K. Padmanabhan¶, Degang Zhong‡, Maria Mastri‖, and Philip J. Fay‖

From the ‡Department of Medicine, Saint Louis University School of Medicine, St. Louis, Missouri 63104, the ¶Department of Biochemistry, Michigan State University, East Lansing, Michigan 48824, and the ‖Department of Biochemistry and Biophysics, University of Rochester School of Medicine, Rochester, New York 14642

The physiologic activator of factor X consists of a complex of factor IXa, factor VIIIa, Ca^{2+} and a suitable phospholipid surface. In one study, helix 330 (162 in chymotrypsin) of the protease domain of factor IXa was implicated in binding to factor VIIIa. In another study, residues 558–565 of the A2 subunit of factor VIIIa were implicated in binding to factor IXa. We now provide data, which indicate that the helix 330 of factor IXa interacts with the 558–565 region of the A2 subunit. Thus, the ability of the isolated A2 subunit was severely impaired in potentiating factor X activation by IXa_{R333Q} and by a helix replacement mutant ($IXa_{helixVII}$ in which helix 330–338 is replaced by that of factor VII) but it was normal for an epidermal growth factor 1 replacement mutant (IXa_{PCEGF1} in which epidermal growth factor 1 domain is replaced by that of protein C). Further, affinity of each 5-dimethylaminonaphthalene-1-sulfonyl (dansyl)-Glu-Gly-Arg-IXa (dEGR-IXa) with the A2 subunit was determined from its ability to inhibit wild-type IXa in the tenase assay and from the changes in dansyl fluorescence emission signal upon its binding to the A2 subunit. Apparent $K_{d(A2)}$ values are: dEGR-IXa_{WT} or dEGR-IXa_{PCEGF1} ~100 nM, dEGR-IXa_{R333Q} ~1.8 μM, and dEGR-$IXa_{helixVII}$ >10 μM. In additional experiments, we measured the affinities of these factor IXa molecules for a peptide comprising residues 558–565 of the A2 subunit. Apparent $K_{d(peptide)}$ values are: dEGR-IXa_{WT} or dEGR-IXa_{PCEGF1} ~4 μM, and dEGR-IXa_{R333Q} ~62 μM. Thus as compared with the wild-type or PCEGF1 mutant, the affinity of the R333Q mutant for the A2 subunit or the A2 558–565 peptide is similarly reduced. These data support a conclusion that the helix 330 of factor IXa interacts with the A2 558–565 sequence. This information was used to model the interface between the IXa protease domain and the A2 subunit, which is also provided herein.

Physiologic blood clotting begins by exposure of blood to tissue factor (TF)[1] at an injury site and formation of the complex between TF and plasma factor VIIa. The TF·VIIa complex formed activates both factors IX and X (1, 2). Factor IXa thus generated forms a stoichiometric complex with factor VIIIa and also activates factor X in the presence of Ca^{2+} and a suitable phospholipid (PL) surface (1, 2). The role of factor VIIIa in this complex is to increase the k_{cat} by several orders of magnitude while PL primarily reduces the K_m for the substrate factor X.

Human factor IX circulates in blood as a single chain protein of 415 amino acids. Upon activation (by factor XIa/Ca^{2+} or TF·VIIa/Ca^{2+}), two peptide bonds in factor IX are cleaved with resultant formation of a serine protease, factor IXa, and release of an activation peptide (3). Factor IXa is composed of a light chain consisting of residues 1–145 and a heavy chain consisting of residues 181–415 of native factor IX, that are held together by a single disulfide bond (4, 5). The light chain of factor IXa consists of an amino-terminal γ-carboxyglutamic acid (Gla)-rich domain (residues 1–40), a short hydrophobic segment (residues 41–46), and two epidermal growth factor (EGF)-like domains (EGF1 residues 47–84 and EGF2 residues 85–127), whereas the heavy chain contains the serine protease domain, which features the catalytic triad residues, namely His^{221} (c57),[2] Asp^{269} (c102), and Ser^{365} (c195) (5). The Gla domain contains several high and low affinity Ca^{2+}-binding sites, whereas EGF1 and protease domain each contain a high affinity Ca^{2+} site (7). For proper binding of factor IXa to PL and factor VIIIa, all of the Ca^{2+} sites in factor IXa must be filled (7, 8).

Factor VIII is synthesized as a single chain molecule containing several domains (A1-A2-B-A3-C1-C2) (9), with a molecular mass of ~300 kDa (10, 11). The A domains are homologous to the ceruloplasmin domains and to the A domains of factor Va (12), whereas the C domains are homologous to the galactose lipid binding domain and to the regions within neuraminidase (13). Factor VIII circulates as a divalent metal ion-dependent, noncovalent heterodimer resulting from proteolytic cleavage at the B/A3 junction that generates a heavy chain (A1-A2-B) and a light chain (A3-C1-C2). This procofactor form is cleaved by thrombin at Arg^{372}-Ser^{373}, Arg^{740}-Ser^{741}, and Arg^{1689}-Ser^{1690}

* This work was supported by National Institutes of Health Grant HL36365 and American Heart Association Grant 9950228N (both to S. P. B.) and by National Institutes of Health Grants HL30616 and HL38199 (to P. J. F.). The costs of publication of this article were defrayed in part by the payment of page charges. This article must therefore be hereby marked "*advertisement*" in accordance with 18 U.S.C. Section 1734 solely to indicate this fact.

§ To whom correspondence should be addressed: Div. of Hematology and Oncology, Saint Louis University Health Sciences Center, 3635 Vista Ave., P.O. Box 15250, St. Louis, MO 63110-0250. Tel.: 314-577-8499/8854; Fax: 314-773-1167; E-mail: bajajps@slu.edu.

[1] The abbreviations used are: TF, tissue factor; Gla, γ-carboxyglutamic acid; EGF, epidermal growth factor; PL, phospholipid; BSA, bovine serum albumin; WT, wild type; TBS, Tris-buffered saline; dansyl, 5-dimethylaminonaphthalene-1-sulfonyl; dEGR-ck, dansyl-Glu-Gly-Arg-chloromethyl ketone; dEGR-IXa, IXa inactivated with dEGR-ck; S-2222, benzoyl-Ile-Glu-Gly-Arg-*p*-nitroanilide; NP, normal plasma; $K_{d(A2)}$, dissociation constant for dEGR-IXa and the A2 subunit; $K_{d(peptide)}$, dissociation constant for factor IXa and the A2 558–565 peptide; TBS, Tris-buffered saline; PAGE, polyacrylamide gel electrophoresis.

[2] For comparison, the factor IX amino acid numbering system is used. The numbers with a prefix c (*e.g.* c57) in parentheses refer to the chymotrypsin equivalents for the protease domain of factor IXa (6).

This paper is available on line at http://www.jbc.org

This is an Open Access article under the CC BY license.

to yield factor VIIIa, a heterotrimer composed of A1, A2, and A3-C1-C2 subunits (14, 15). The A1 and A3-C1-C2 subunits remain associated with a divalent metal ion-dependent linkage, whereas the A2 subunit is weakly associated with the A1 and A3-C1-C2 dimer (16, 17). Although intact factor VIIIa is required for maximal enhancement of factor IXa activity, recent results demonstrate that the isolated A2 subunit stimulates factor IXa activity by ~100-fold (18).

Ca^{2+}-dependent assembly of factor IXa and factor VIIIa on a suitable PL surface is essential for hemostasis since defects or deficiency in the proteins result in severe bleeding diatheses, namely hemophilia A (factor VIII deficiency) or hemophilia B (factor IX deficiency) (Ref. 12; see the hemophilia A mutation data base and the Haemophilia B data base of point mutations and short additions and deletions, both available via the World Wide Web). In this assembly, the Ca^{2+}-loaded form of the Gla domain of factor IXa binds to PL (21), whereas EGF1[3]/EGF2 region(s) and the protease domain are thought to interact with the A3 and A2 subunits of factor VIIIa, respectively (18, 22). Factor VIIIa in this assembly anchors to the PL surface via its C2 domain (13), and binding of factor X to the IXa/VIIIa complex may be partly mediated through the A1 subunit of factor VIIIa (23).

In the IXa/VIIIa complex, residues 558–565 of the A2 subunit of factor VIIIa are thought to bind to the protease domain of factor IXa (24). Further, helix 330–338 (c162–170) of the protease domain of factor IXa has been shown to bind to factor VIIIa (25). However, whether or not helix 330–338 of factor IXa binds to the A2 subunit or more specifically to its 558–565 peptide region is not known. The present study is designed to address this issue. The kinetic, fluorescence, and inhibition data indicate that helix 330 (c162) of factor IXa most likely interacts with the 558–565 region of the A2 subunit. An interface model between the helix 330–338 of factor IXa and the A2 558–565 region was then constructed. Other spatially nearby residues in factor IXa as well as those in the A2 subunit that could contribute to the interface were noted. The role of these residues in this interaction is discussed.

EXPERIMENTAL PROCEDURES

Reagents—Benzoyl-Ile-Glu-Gly-Arg-*p*-nitroanilide (S-2222) was purchased from Helena Laboratories. Dansyl-Glu-Gly-Arg-chloromethyl ketone (dEGR-ck) was obtained from Calbiochem. Phosphatidylcholine, phosphatidylserine, phosphatidylethanolamine, recombinant hirudin, and fatty acid-free bovine serum albumin (BSA) were obtained from Sigma. PL vesicles containing 75% phosphatidylcholine and 25% phosphatidylserine were prepared by the method of Husten *et al*. (26) and used for all experiments except for the fluorescence emission studies. For fluorescence experiments, PL vesicles comprised 40% phosphatidylcholine, 20% phosphatidylserine, and 40% phosphatidylethanolamine and were prepared using octyl glucoside as described (27). Recombinant factor VIII preparations (Kogenate®) were a gift from Drs. Lisa Regan and Jim Brown of Bayer Corp.. Purified recombinant factor VIII was also a generous gift from Debra Pittman of the Genetics Institute. Normal plasma factor IX (IX_{NP}) and factor X were isolated as described (6), and factor Xa was prepared as outlined (28). Purified human factor XIa and α-thrombin were purchased from Enzyme Research Laboratories (South Bend, IN). A synthetic peptide corresponding to the A2 subunit residues 558–565 (Ser-Val-Asp-Gln-Arg-Gly-Asn-Gln) was obtained as described previously (18), and its concentration was determined by amino acid analysis.

Proteins—The Kogenate® concentrate was fractionated to separate factor VIII from albumin following S-Sepharose chromatography as outlined (29). Factor VIIIa was prepared from factor VIII using thrombin and subsequently purified using CM-Sepharose chromatography (30), and the A2 subunit and A1/A3-C1-C2 dimer were separated by Mono S chromatography (15). The A2 subunit was further purified using an anti-A2 immunoaffinity column (15). The purified A2 subunit was essentially homogeneous (>95% pure), as judged by SDS-PAGE. For some experiments, proteins were concentrated using a Microcon concentrator (Millipore, 10-kDa cut-off). The concentration of the A2 subunit was determined by the Coomassie Blue dye binding method of Bradford (31). Wild-type factor IX (IX_{WT}), as well as mutants IX_{R333Q} (a point mutant in which R333 is replaced by Gln), $IX_{VIIhelix}$ (a replacement mutant in which helix 330–338 (c162–170) is replaced by that of factor VII), and IX_{PCEGF1} (a replacement mutant in which EGF1 domain is replaced by that of protein C), were constructed, expressed, and purified as described previously (25, 32, 33). Purified proteins were homogeneous on SDS-PAGE and contained normal Gla content (25, 32).

Preparation of dEGR-ck-inhibited Factor IXa Proteins—Each factor IX protein was activated at 200 μg/ml by factor XIa (2 μg/ml) for 90 min. The buffer used was TBS, pH 7.5 (50 mM Tris, 150 mM NaCl, pH 7.5), containing 5 mM $CaCl_2$. SDS-PAGE analysis revealed full activation of each factor IX to factor IXa without degradation in the autolysis loop (34). dEGR-IXa_{WT} and various dEGR-IXa mutant proteins free of dEGR-ck were obtained as described previously (34).

Activation of Factor X by Each Factor IXa Protein in the Presence of Ca^{2+} and PL—For these studies, each factor IX was activated with factor XIa/Ca^{2+} as described above. For factor X activation studies, the concentration of factor IXa was kept at 20 nM and the buffer used was TBS/BSA (TBS with 200 μg/ml BSA) containing 5 mM $CaCl_2$. The concentrations of PL used were 10, 25, 50, and 100 μM in different sets of experiments. The concentration of factor X at each PL concentration ranged from 25 nM to 3 μM. The activations were carried out for 5–15 min, and the amount of factor Xa generated was measured by hydrolysis of S-2222 as described previously (25, 34). The K_m and k_{cat} values were obtained using the program GraFit from Erithacus Software.

Determination of EC_{50} of Interaction of factor IXa Proteins with the A2 Subunit—The EC_{50} (functional K_d) of binding of each factor IXa protein with the A2 subunit was measured essentially as described previously for its interaction with the intact factor VIIIa (25, 34). For these experiments, concentrations of factor IXa and factor X were kept constant, and the rates of formation of factor Xa were determined at increasing concentrations of the A2 subunit. Reaction mixtures contained 5 nM factor IXa, 250 nM factor X, 25 μM PL, and various concentrations of the A2 subunit in TBS/BSA, pH 7.5 containing 5 mM $CaCl_2$. Reactions were carried out at 37 °C for 5–20 min and stopped by adding 1 μl of 500 mM EDTA. The amount of factor Xa generated was determined by S-2222 hydrolysis as described previously (25, 34). The EC_{50} was obtained by fitting the data to a single-site ligand binding equation (Equation 1) by non-linear regression analysis using the program GraFit from Erithacus Software.

$$V = \frac{V_{max}L}{EC_{50} + L} \quad \text{(Eq. 1)}$$

V is the rate of formation of factor Xa at a given concentration of the A2 subunit, denoted by L, and V_{max} is the rate of factor Xa formation by the factor IXa:A2 subunit complex. EC_{50} is the functional K_d defined as the concentration of free A2 subunit yielding 50% of the V_{max}. The background rate of factor Xa generation was obtained by carrying out the reaction in the absence of the A2 subunit. This represented less than 1% of the V_{max} and was subtracted before data analysis. To obtain EC_{50} values as a function of substrate concentration, a series of experiments were performed in which factor X was varied from 50 nM to 1 μM.

Determination of the Apparent $K_{d(A2)}$ of Binding of dEGR-IXa Proteins to the A2 Subunit—The apparent K_d (termed $K_{d(A2)}$) for binding of each dEGR-IXa protein to the A2 subunit was determined by its ability to inhibit factor IXa_{WT}:A2 subunit interaction in the tenase complex as described previously for intact factor VIIIa (25, 34). The reactions were carried out as described for the EC_{50} experiments above, except that the dEGR-IXa and IXa_{WT} were mixed prior to addition of the A2 subunit; this ensured steady state conditions. Mixtures contained 100 nM IXa_{WT}, 30 nM A2 subunit, 250 nM factor X, 25 μM PL, and various concentrations of dEGR-IXa proteins in TBS/BSA, pH 7.5 containing 5 mM $CaCl_2$. The IC_{50} (concentration of inhibitor required for 50% inhibition) was determined by fitting the data to IC_{50} four-parameter logistic equation of Halfman (35) given below.

$$y = \frac{a}{1 + (x/IC_{50})^s} + \text{background} \quad \text{(Eq. 2)}$$

y is the rate of factor Xa formation in the presence of a given concentration of dEGR-IXa protein represented by x, a is the maximum rate of

[3] Although there is a considerable controversy as to the role of EGF1 domain in the interaction of factor IXa and factor VIIIa, at present it cannot be completely ruled out that this domain contains a direct interactive site for factor VIIIa (8).

factor Xa formation in the absence of dEGR-IXa, and *s* is the slope factor. Each point was weighted equally, and the data were fitted to Equation 2 using the nonlinear regression analysis program GraFit from Erithacus Software. The background value represented ~5% of the maximum rate of factor Xa formation in the absence of dEGR-IXa. To obtain apparent $K_{d(A2)}$ values for the interaction of dEGR-IXa proteins with A2, we used the following equation as described by Cheng and Prusoff (36) and further elaborated by Craig (37).

$$K_{d(A2)} = \frac{IC_{50}}{1 + (A/EC_{50})} \quad \text{(Eq. 3)}$$

A is the concentration of factor IXa_{WT}, and EC_{50} is the concentration of factor IXa_{WT} that gives a 50% maximum response in the absence of the competitor at a specified concentration of factor X used in the experiment.

Fluorescence Quenching of the Dansyl Moiety in dEGR-IXa by the A2 Subunit—Effect of the A2 subunit on the emission intensity of the dansyl moiety in each dEGR-IXa protein was determined using the SLM AB2 spectrofluorometer. Each reaction mixture contained 220 nM dEGR-IXa in 20 mM Hepes, pH 7.2, 100 mM NaCl, 5 mM $CaCl_2$, 0.01% Tween, 200 μg/ml BSA, and 100 μM PL vesicles. The excitation wavelength was 340 nm (slit width, 8 nm) and the emission wavelength was 540 nm (slit width, 8 nm). First, blank values (in triplicate) were obtained for the buffer containing PL. dEGR-IXa was then added, and the emission intensity in the absence of the A2 subunit was recorded. Each reaction mixture was subsequently titrated with the A2 subunit, and the emission readings (in triplicate) were obtained at each point. The fluorescence emission intensity at each point was corrected for increases in the reaction volume prior to analysis of the data. The volume of added A2 subunit did not exceed 10% of the total volume. Data are presented as F/F_0, where F_0 is the emission intensity in the absence of A2 subunit and *F* is the intensity at a given A2 subunit concentration.

Determination of the Apparent $K_{d(peptide)}$ of binding of each factor IXa to the A2 558–565 peptide—The apparent K_d (termed $K_{d(peptide)}$) for binding of each factor IXa to the A2 558–565 peptide was determined by its ability to inhibit the respective IXa:A2 subunit interaction, as measured by reduction in the rate of factor X activation in the tenase system. The reaction mixtures for both IXa_{WT} and IXa_{PCEGF1} contained 100 nM factor IXa, 30 nM A2 subunit, 250 nM factor X, and 25 μM PL in TBS/BSA, pH 7.5, with 5 mM $CaCl_2$. The reaction mixture for IXa_{R333Q} contained 300 nM factor IXa instead of 100 nM used for IXa_{WT} or IXa_{PCEGF1}; concentrations of other components were the same. The amount of factor Xa generated was determined by hydrolysis of S-2222. The IC_{50} values were obtained using Equation 2. Here, *y* is the rate of factor Xa formation in the presence of a given concentration of the A2 558–565 peptide represented by *x*, and *a* is the maximum rate of factor Xa formation in the absence of the A2 peptide. Equation 3 was then used to obtain the apparent $K_{d(peptide)}$ values. Here, *A* is the concentration of IXa_{WT}, IXa_{PCEGF1}, or IXa_{R333Q}, and EC_{50} is the apparent $K_{d(A2)}$ for the respective IXa:A2 subunit interaction.

Molecular Modeling—The three (A1, A2, and A3) domains in factor VIIIa are homologous to the three respective domains in ceruloplasmin (12, 38). The A1, A2, and A3 domains of factor VIIIa were modeled using the coordinates of each respective domain of ceruloplasmin (39). Each domain was modeled using the homology model building module from Biosym/MSI (San Diego, CA), as well as the Swiss-Model server using the optimize mode (40, 41). The two approaches used in building the homology models resulted in minor differences between the structure of each of the A subunits. However, the structure pertaining to the loop containing the 3_{10} helical turn involving residues 558–565 as well as other nearby interface regions of the A2 subunit implicated in binding to factor IXa were invariant between the two models. Further, the Biosym/MSI models of all three A subunits were similar to those published previously by Pemberton *et al*. (12). Thus, we used the coordinates of Pemberton *et al.* (Ref. 12; see hemophilia data base, available on-line) in building the interface between the A2 subunit and the protease domain of factor IXa. Details are provided under "Results and Discussion."

RESULTS AND DISCUSSION

Activation of Factor X by Various Factor IXa Proteins in the Presence of Only Ca^{2+} and PL—The kinetic constants for the activation of factor X were obtained by various factor IXa proteins in the presence of Ca^{2+} and several concentration of PL. This analysis was performed to establish whether or not the factor IXa proteins under investigation bind to Ca^{2+} and PL normally and possess a functional active site. The kinetic constants obtained under these conditions in the absence of factor VIIIa are listed in Table I. All mutants activated factor X normally, and the specificity constant (kcat/K_m) for each mutant at different PL concentrations did not differ appreciably from that observed for IXa_{WT} or IXa_{NP}. The increase in K_m values at higher concentrations of PL for WT or for a given mutant may reflect binding of factor IXa and factor X to different PL vesicles (42, 43). Further, our K_m and k_{cat} values are in close agreement with the earlier published data (18, 43). Consistent with earlier observations (43), we also observed a slight increase in k_{cat} for each factor IXa protein at higher concentrations of PL. Cumulatively, our data presented in Table I indicate that the factor IXa mutants under investigation interact with Ca^{2+} and PL normally. Further, in the absence of factor VIIIa, activation of factor X by these IXa mutants is not impaired.

TABLE I
Kinetic parameters of factor X activation in the absence of factor VIIIa

Concentration of each reagent in the reaction mixture was: 20 nM factor IXa, 5 mM $CaCl_2$, and varying concentrations of factor X ranging from 25 nM to 3 μM.

Protein	PL	K_m	k_{cat}	k_{cat}/K_m
	μM	μM	min^{-1}	$\mu M^{-1}\ min^{-1}$
IXa_{NP}	10	0.10	0.012	0.108
	25	0.16	0.022	0.138
	50	0.21	0.032	0.156
	100	0.63	0.062	0.098
IXa_{WT}	10	0.09	0.010	0.110
	25	0.12	0.012	0.102
	50	0.24	0.024	0.100
	100	0.57	0.038	0.066
IXa_{PCEGF1}	10	0.13	0.010	0.076
	25	0.23	0.018	0.080
	50	0.26	0.028	0.110
	100	0.54	0.038	0.070
IXa_{R333Q}	10	0.11	0.012	0.108
	25	0.18	0.018	0.100
	50	0.23	0.030	0.130
	100	0.61	0.040	0.066
$IXa_{VIIhelix}$	10	0.12	0.014	0.116
	25	0.20	0.020	0.100
	50	0.25	0.028	0.112
	100	0.55	0.042	0.076

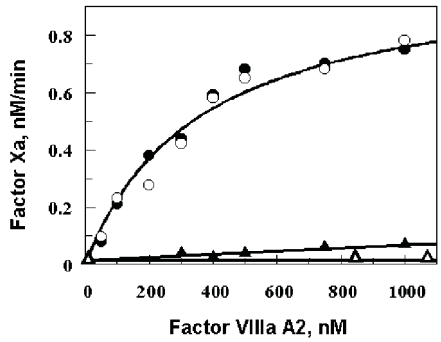

FIG. 1. **Effect of the isolated A2 subunit of factor VIIIa on the rate of activation of factor X by various factor IXa proteins.** Rate of formation of factor Xa by each factor IXa protein was measured as described under "Experimental Procedures." The reaction mixtures contained 5 nM factor IXa, 250 nM factor X, and various concentrations of A2 subunit. The buffer used was TBS/BSA, pH 7.5 containing 25 μM PL and 5 mM $CaCl_2$. The proteins used are: IXa_{WT} (*closed circles*), IXa_{PCEGF1} (*open circles*), IXa_{R333Q} (*closed triangles*), and $IXa_{VIIhelix}$ (*open triangles*). The data were fitted to a single-site binding equation (Equation 1).

A2 Subunit-mediated Enhancement of Factor X Activation by Various Factor IXa Mutants—In this section, we evaluated the

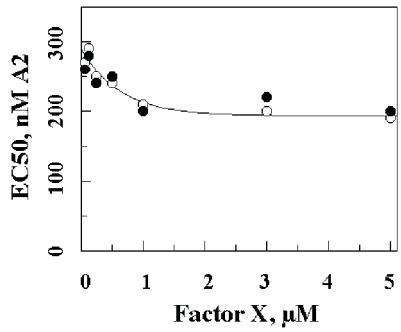

FIG. 2. **Effect of factor X concentration on the EC_{50} (functional K_d) of the interaction of A2 subunit with IXa_{WT} or IXa_{PCEGF1}.** The EC_{50} of the interaction of factor IXa_{WT} (*closed circles*) or factor IXa_{PCEGF1} (*open circles*) with the A2 subunit was determined at various concentrations of factor X. Each point (EC_{50}) shown is the concentration of free A2 subunit (*y* axis) providing 50% of the V_{max}. Each EC_{50} value was obtained from a direct plot (similar to Fig. 1) of factor Xa generation at various concentrations of the A2 subunit and a constant concentration of factor X. The factor IXa concentration in each experiment was fixed at 5 nM. The buffer used was TBS/BSA, pH 7.5, containing 25 μM PL and 5 mM $CaCl_2$. Factor Xa concentration was measured by S-2222 hydrolysis.

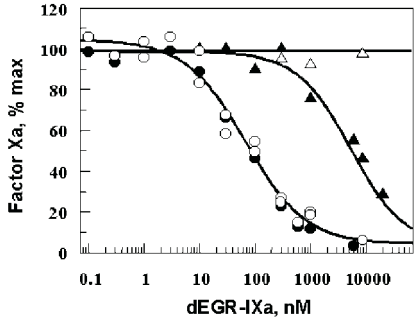

FIG. 3. **Abilities of various dEGR-IXa proteins to inhibit factor IXa:A2 subunit interaction as measured by a decrease in factor Xa generation in the tenase system.** The reaction mixtures contained 100 nM IXa_{WT}, 30 nM A2 subunit, 250 nM factor X, 25 μM PL, and various concentrations of dEGR-IXa proteins in TBS/BSA, pH 7.5, containing 5 mM $CaCl_2$. Factor Xa generation was measured by S-2222 hydrolysis. The value of slope factor, *s*, was 0.9 ± 0.1, indicating a single affinity binding site between the interacting proteins. The *curves* represent best fit of the data to the IC_{50} four-parameter logistic equation (Equation 2). The proteins used are: dEGR-IXa_{WT} (*closed circles*), dEGR-IXa_{PCEGF1} (*open circles*), dEGR-IXa_{R333Q} (*closed triangles*), and dEGR-$IXa_{VIIhelix}$ (*open triangles*). The inhibition curve obtained with dEGR-IXa_{NP} was similar to that depicted for dEGR-IXa_{WT} (graph not shown).

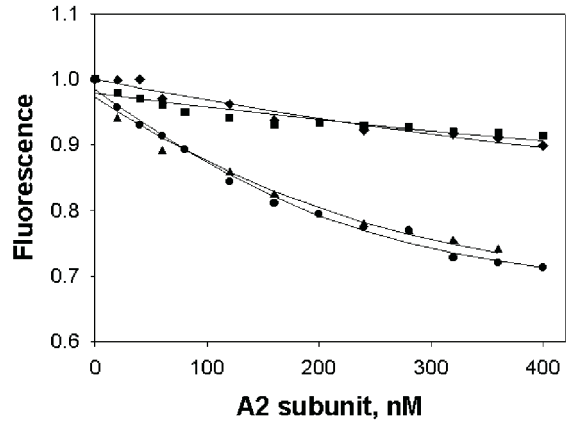

FIG. 4. **Effect of the A2 subunit on the fluorescence emission intensity of dEGR-IXa proteins.** Reactions (160 μl) were titrated with A2 subunit in buffer containing 20 mM Hepes, pH 7.2, 100 mM NaCl, 5 mM $CaCl_2$, 0.01% Tween 20, 200 μg/ml BSA, and 100 μM PL vesicles. Fluorescence emission intensity of each dEGR-IXa (220 nM) at a given A2 subunit concentration was determined as described under "Experimental Procedures." Data were fitted to a bimolecular association model and are presented as F/F_0, where F_0 is the emission intensity in the absence and F is the emission intensity at a given A2 subunit concentration. dEGR-IXa_{WT} (*triangles*), dEGR-IXa_{PCEGF1} (*circles*), dEGR-IXa_{R333Q} (*diamonds*), and dEGR-$IXa_{VIIhelix}$ (*squares*).

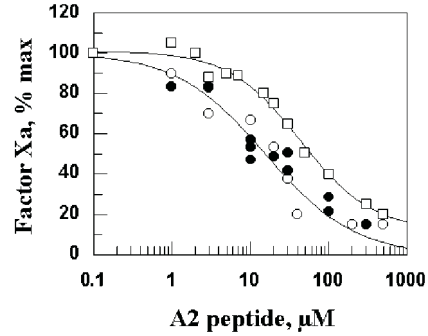

FIG. 5. **Ability of the 558–565 A2 peptide to inhibit the interaction of various factor IXa proteins with the A2 subunit.** The reaction mixture for factor IXa_{WT} (*closed circles*) or factor IXa_{PCEGF1} (*open circles*) contained 100 nM of factor IXa protein, 30 nM A2 subunit, 250 nM factor X, 5 mM $CaCl_2$, and 25 μM PL in TBS/BSA, pH 7.5. The reaction mixture for factor IXa_{R333Q} (*open squares*) contained 300 nM factor IXa instead of 100 nM used for factor IXa_{WT} or factor IXa_{PCEGF1}; the concentrations of other components were unchanged. Factor Xa generation was determined by S-2222 hydrolysis, and the *curves* represent best fit to the IC_{50} four-parameter logistic equation (Equation 2). The value of slope factor, *s*, was 0.9 ± 0.1, indicating a single affinity binding site between the various IXa proteins and the A2 peptide.

ability of the A2 subunit to augment factor X activation by various factor IXa mutants. These data are presented in Fig. 1. The presence of the A2 subunit in the reaction mixtures enhanced the factor X-activating activity of IXa_{PCEGF1} to the same extent as that of IXa_{WT}. However, the ability of the A2 subunit to potentiate the activity of IXa_{R333Q} was severely impaired, and it was essentially absent for $IXa_{VIIhelix}$. Next, we determined the EC_{50} (functional K_d) values for interaction of each factor IXa protein with the A2 subunit using Eq. 1. Fitting the data to a single-site binding model yielded an apparent $K_{d(A2)}$ of 257 ± 31 for both IXa_{WT} and IXa_{PCEGF1}; for IXa_{R333Q} or $IXa_{VIIhelix}$, it could not be calculated. These data indicate that the helix 330 (c162) of factor IXa interacts with the A2 subunit of factor VIIIa.

In further experiments, we measured the EC_{50} values for interaction of IXa_{WT} and of IXa_{PCEGF1} with the A2 subunit using different concentrations of factor X ranging from 50 nM to 5 μM. These data are presented in Fig. 2. At each concentration of factor X, the concentration of factor IXa was held constant at 5 nM and the rate of factor Xa generation was determined in the presence of increasing concentrations of the A2 subunit. The EC_{50} values ranged from ~280 nM at lower concentrations of factor X (<150 nM) to ~200 nM at higher concentrations of factor X (>1 μM) for both IXa_{WT} and IXa_{PCEGF1}. Our functional K_d (EC_{50}) values ranging from 200 to 280 nM for the interaction of IXa_{WT} (or IXa_{PCEGF1}) and the A2 subunit employing different factor X concentrations are consistent with the EC_{50} values obtained earlier using similar conditions for IXa_{NP} and the A2 subunit (18). From these observations, we conclude that factor X does not appreciably influence the functional K_d of IXa:A2 subunit interaction. This is in contrast to the results obtained using factor VIIIa where factor X reduces the functional K_d of IXa:VIIIa interaction by ~10-fold (34). These results support previous observations that the A1 subunit of factor VIIIa interacts with factor X (23). More importantly, our data with the IXa_{PCEGF1} mutant indicate that the EGF1 domain of factor IXa does not interact with the A2 subunit of factor VIIIa.

TABLE II

Apparent K_d and Gibbs free energy values for the interaction of various factor IXa proteins with the A2 subunit and the A2 558–565 peptide

Apparent $K_{d(A2)}$ values are from Fig. 3, and apparent $K_{d(peptide)}$ values are from Fig. 5.

Protein	Apparent $K_{d(A2)}$	ΔG^0_{A2} [b]	Apparent $K_{d(peptide)}$	$\Delta G^0_{peptide}$ [b]
	nM	*kcal mol^{-1}*	*μM*	*kcal mol^{-1}*
IXa_{WT}	100 ± 11	9.54	4 ± 1	7.36
IXa_{PCEGF1}	114 ± 15 (1)[a]	9.47 (0.07)[c]	4 ± 1 (1)[a]	7.36 (0.00)[c]
IXa_{R333Q}	1850 ± 82 (18)	7.82 (1.72)	62 ± 9 (15)	5.74 (1.62)
$IXa_{VIIhelix}$	>10^4	ND[d]	ND	ND

[a] The -fold change in apparent K_d values (mutant/WT) is given in parentheses.
[b] Gibbs free energy values were calculated using the equation, $\Delta G^0 = -RT\ln K_d$, where R is the gas constant (1.987×10^{-3} kcal mol^{-1} deg^{-1}), T is the absolute temperature (298 K), and K_d is the dissociation constant.
[c] The change in ΔG^0 values between the mutant and WT is given in parentheses.
[d] ND, not determined.

Determination of Apparent $K_{d(A2}$ Values for the Interaction of A2 Subunit with dEGR-IXa Proteins—Here, we investigated the steady state inhibition of IXa_{WT}:A2 subunit interaction by different dEGR-IXa proteins. These data are presented in Fig. 3. The IC_{50} values were obtained using Equation 2, and the respective apparent $K_{d(A2)}$ values were obtained using Equation 3. dEGR-IXa_{WT} and dEGR-IXa_{PCEGF1} interacted with the A2 subunit with a similar $K_{d(A2)}$ of ~100 nM, whereas dEGR-IXa_{R333Q} interacted with the A2 subunit with a $K_{d(A2)}$ of ~1.8 μM and dEGR-$IXa_{VIIhelix}$ failed to compete with factor IXa_{WT} up to 12 μM concentration. The apparent $K_{d(A2)}$ (~100 nM) obtained from the inhibition data (Fig. 3) and EC_{50} values (200–280 nM) obtained from the potentiation of factor X activation data (Figs. 1 and 2) for the factor IXa_{WT} and IXa_{PCEGF1} are in close agreement with each other. Of significance is the observation that the mutations in the helix 330 (c162) of the protease domain of factor IXa severely impairs its interaction with the A2 subunit.

Effects of the A2 Subunit on the Fluorescence Emission of dEGR-IXa Proteins—Since dansyl emission is quite sensitive to its environment, we examined the changes in dansyl emission intensity (excitation wavelength, 340 nm; emission wavelength, 540 nm) of dEGR-IXa proteins in the presence of increasing concentrations of the A2 subunit. Reaction mixtures contained 220 nM amounts of each dEGR-IXa protein, 100 μM PL, and various concentrations of the isolated A2 subunit. The results are presented in Fig. 4. For IXa_{WT} or IXa_{PCEGF1}, a dose-dependent decrease in the fluorescence emission of the dansyl probe was observed. However, little if any change in the emission intensity was observed when the A2 subunit was titrated into the reaction mixtures containing factor IXa_{R333Q} or $IXa_{VIIhelix}$. A nonlinear least squares fitting of the data for IXa_{WT} and IXa_{PCEGF1} to a bimolecular association model yielded a plateau value of 0.59 ± 0.05 for F/F_0 and an apparent $K_{d(A2)}$ value of 82 ± 18 nM for each protein. Further, the $K_{d(A2)}$ for IXa_{R333Q} or $IXa_{VIIhelix}$ could not be calculated. These results suggest that the isolated A2 subunit interacts equivalently with IXa_{WT} and IXa_{PCEGF1}, and similarly modulates the emission of the active site-labeled dansyl probe. The apparent $K_{d(A2)}$ value of ~82 nM for factor IXa_{WT} or IXa_{PCEGF1} obtained using the fluorescence quenching measurements is in agreement with the values obtained from steady state inhibition experiments. Consistent with the data presented in Figs. 1 and 3, these fluorescence results suggest that the factor IXa_{R333Q} and $IXa_{VIIhelix}$ mutants are severely impaired in their interactions with the A2 subunit.

Determination of Apparent K_d Peptide Values for Binding of Factor IXa Proteins to the A2 558–565 Peptide—The data presented thus far strongly indicate that the A2 subunit interacts with residues of the helix 330 (c162) of factor IXa. Previous studies also suggest that residues 558–565 of the A2 subunit are involved in binding to factor IXa (18). However, it is not known whether the 558–565 peptide region of the A2 subunit represents the site of direct interaction with the helix 330 of factor IXa. We investigated this possibility by measuring the affinity of the A2 558–565 peptide for IXa_{WT}, IXa_{PCEGF1}, and IXa_{R333Q}. These data are presented in Fig. 5. The A2 558–565 peptide inhibits the interaction of IXa_{WT} and IXa_{PCEGF1} with similar IC_{50} values of ~8 μM.[4] However, the A2 558–565 peptide inhibited the IXa_{R333Q}:A2 subunit interaction with an IC_{50} value of ~70 μM, which is ~9-fold higher than the value obtained for IXa_{WT} or IXa_{PCEGF1} (Fig. 5). We next used the Cheng and Prusoff relationship (36, 37) to obtain apparent $K_{d(peptide)}$ values for each factor IXa protein. These apparent $K_{d(peptide)}$ values along with the changes in Gibbs free energy are listed in Table II. The peptide bound to IXa_{WT} and IXa_{PCEGF1} with an apparent K_d of ~4 μM and to IXa_{R333Q} with an apparent K_d of ~62 μM. Thus, the affinity of the A2 558–565 peptide for IXa_{WT} and IXa_{PCEGF1} is similar, whereas it is reduced ~15-fold for the IXa_{R333Q}.

Notably, comparison of the data presented in Figs. 3 and 5 reveal that the increase in apparent $K_{d(A2)}$ or $K_{d(peptide)}$ for IXa_{R333Q} is similar as compared with the apparent $K_{d(A2)}$ or $K_{d(peptide)}$ obtained for IXa_{WT} (or IXa_{PCEGF1}). Further, the difference in ΔG^0 for the interaction of A2 subunit with IXa_{WT} (or IXa_{PCEGF1}) and IXa_{R333Q} is 1.72 kcal mol^{-1} (Table II). This difference in ΔG^0 is essentially the same as that (1.62 kcal mol^{-1}) obtained for the interaction of A2 peptide with IXa_{WT} (or IXa_{PCEGF1}) and IXa_{R333Q}. If the A2 558–565 peptide bound to a different region than the helix 330 of factor IXa, then one would expect it to bind to IXa_{R333Q} with the same affinity as that for IXa_{WT}. Since this is not the case, our data support a conclusion that the helix 330 (c162) in factor IXa is most likely in direct contact with the 558–565 region of the A2 subunit.

Modeling of the Interface between the Protease Domain of Factor IXa and the A2 Subunit of Factor VIIIa—Based upon the preceding information, we modeled the interface between the protease domain of factor IXa (Ref. 5, Protein Data Bank code 1RFN) and the A2 subunit (see "Experimental Procedures") by bringing together the helix 330 of factor IXa and the 3_{10} helical turn in residues 558–565 of the A2 subunit and maximizing the interaction among the charged residues. Emphasis was also given for interactions involving hydrogen bonds and hydrophobic contacts. An important guiding principle in the construction of this interface model was that the Gla domain of factor IXa and the C2 domain of factor VIIIa must be oriented such that each may contact the PL surface. To achieve

[4] The present IC_{50} value (~8 μM) for the A2 peptide inhibition of the IXa_{WT}:A2 subunit interaction is 5-fold lower than the IC_{50} value (~40 μM) obtained from the inhibition studies of the A2 subunit enhancement of IXa_{NP} activity (18). This difference in IC_{50} values is most likely due to the different concentrations (30 nM in present study *versus* 240 nM in previous study) of the A2 subunit used in the two studies.

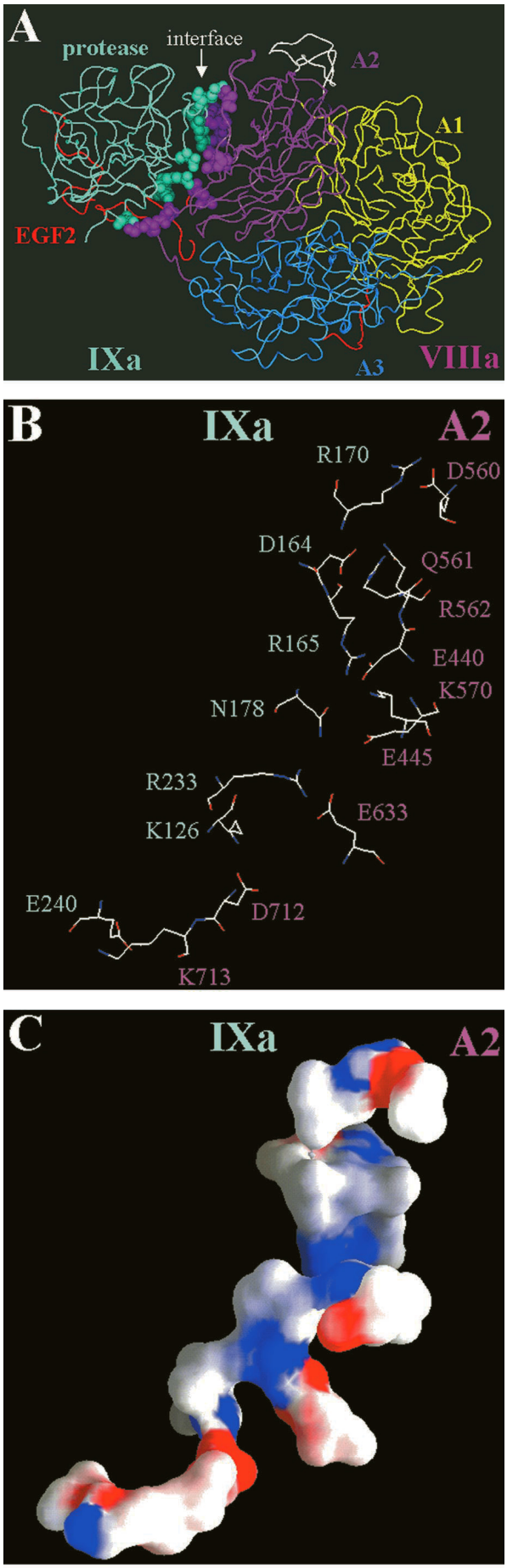

this, the A2 structure (along with the A1 and A3 subunits) was rotated and translated as a rigid body. The principle approach used was that described earlier by Tulinsky and co-workers (44) in building the prothrombin model from the structures of prothrombin fragment 1 and the fragment 2-thrombin complex. Minor adjustments in the side chains of both proteins were also made. All residues in the interface of both proteins were checked for distances to ensure no improper contacts (45). The interface model that resulted from this approach is shown in Fig. 6*A*. In this display, the Gla domain of factor IXa and the C2 domain of factor VIIIa are projecting away from the viewer.

In addition to the A2 558–565 region and the factor IXa 330–338 region, other spatially nearby regions that may play important roles in the interaction of A2 subunit with the protease domain were also noted. The details of the composite interface region are shown in Fig. 6*B*. It appears that electrostatic forces might play a significant role in the interaction between the A2 subunit and the protease domain, and an electrostatic potential for the interface calculated using the program GRASP (46) is shown in Fig. 6*C*. Further, in addition to the electrostatic interactions outlined in Fig. 6, hydrophobic and polar uncharged interactions between Thr^{343} (c175) and Tyr^{345} (c177) of factor IXa and His^{444} of the A2 subunit were observed. Moreover, a hydrogen bond between Asn^{258} (c93) of factor IXa and Ser^{709} of the A2 subunit could also be formed. Importantly, a significant hydrophobic patch involving Ile^{566} and Met^{567} in the A2 subunit and Ile^{298} (c129B), Tyr^{295} (c128), Phe^{299} (c130), Phe^{302} (c133), Phe^{378} (c208), and Phe^{98} (EGF2 domain) in factor IXa was noted. Thus, it appears that the hydrogen bonds as well as the hydrophobic and electrostatic interactions all play important roles in the proposed interface between factor IXa and the A2 subunit. In this context, an apparent $K_{d(A2)}$ of ~100 nM observed for this interaction reflects the net change in free energy involved in making and breaking such bonds.

A factor IXa-interactive site comprising residues 484–509 in the A2 subunit that was identified using a monoclonal antibody (47) does not appear to contact the protease domain in our interface model. However, it should be noted that, in a previous study (48), Lollar *et al.* concluded that this same monoclonal antibody does not interfere with the IXa:VIIIa interaction. The

Fig. 6. **Interface model between the factor IXa protease domain and the A2 subunit of factor VIIIa.** The coordinates for the human factor IXa structure are from the Brookhaven Protein Data Bank (code 1RFN) and the coordinates for the A1, A2, and A3 subunits (12) of factor VIIIa are based upon homology models built using ceruloplasmin coordinates (Protein Data Bank code 1KCW). *A*, schematic representation of the interface model. Ribbon structure for each protein is depicted. The IXa protease domain is in *light blue*, and the EGF2 domain is in *red*. The A1 subunit is in *yellow*, the A2 subunit is in *magenta* with residues 484–509 in *white*, and the A3 subunit is in *cyan* with the COOH terminus in *red*. The Gla and the EGF1 domains of factor IXa and the C1 and C2 domains of factor VIIIa are not shown. The interface residues of factor IXa protease domain and of the A2 subunit are shown as CPK space-filling models. The molecules are oriented such that the Gla domain of factor IXa and the C2 domain of factor VIIIa are projecting away from the viewer. The Gla domain in factor IXa and the C2 domain of factor VIIIa bind to the PL surface. *B*, detailed interface between factor IXa protease domain and the modeled A2 subunit. Only the charged residues that participate in the binding interactions are depicted. The hydrophobic residues that participate in this interaction are discussed in the text. The orientation of the molecules is the same as in *A*. Chymotrypsin numbering system for the factor IXa protease domain is used. Corresponding factor IX numbering system are 338 (c170), 332 (c164), 333 (c165), 346 (c178), 403 (c233), 293 (c126), and 410 (c240). Factor IXa residues are labeled *light blue*, and A2 subunit residues are labeled *magenta*. *C*, electrostatic potential between the factor IXa protease domain and the A2 subunit interface as determined using the program GRASP (46). *Blue* represents positive, *red* represents negative, and *white* represents neutral residues.

reason(s) for the differing results obtained in the two studies (47, 48) is not fully understood. Further, in the proposed interface model shown in Fig. 6*A*, the 484–509 region in the A2 subunit is not in close proximity to the 558–565 interface region and shows no apparent contacts with factor IXa. However, we cannot exclude the possibility of a change in the conformation of the A2 subunit upon binding the protease domain, which may juxtapose (and subsequently involve) this region. Alternatively, the monoclonal antibody may prevent the association of the A2 subunit with factor IXa through steric interference.

Analysis of Hemophilia Data Bases—Of significance is the observation that numerous mutations in the helix 330 (c162) of factor IXa cause hemophilia B (see Ref. 25 and the Haemophilia B data base of point mutations and short additions and deletion), whereas several mutations in or near factor VIII residues 558–565 result in hemophilia A (Ref. 12; see hemophilia data base, available on-line). Arg^{333} (c165) in our interface model (Fig. 6) interacts with Glu^{440} residue of the A2 subunit, and mutations in the Arg^{333} (c165) that eliminate the charge (Arg → Gln or Leu) cause severe hemophilia B (see Haemophilia B data base of point mutations and short additions and deletion, available via the World Wide Web). Further, Asn^{346} (c178) of factor IXa interacts with both Lys^{570} and Glu^{445} of the A2 subunit, and a mutation of Asn^{346} (c178) to Asp causes hemophilia B (see Haemophilia B data base). Similarly, Arg^{403} (c233) in our model interacts with Glu^{633} of the A2 subunit and mutations in Arg^{403} (c233) to Trp or Gln cause hemophilia B (see Haemophilia B data base). Moreover, Arg^{338} (c170) of factor IXa interacts with Asp^{560} of the A2 subunit, and mutations in both of these residues result in hemophilia (HAMSTeRS data base and Haemophilia B data base, both available via the World Wide Web). In addition, Arg^{562} contained within the A2 558–565 peptide region is cleaved by activated protein C (17), and factor IXa selectively protects this site from cleavage (49). In support of this observation, Arg^{562} of the A2 subunit along with Gln^{561} interacts with Asp^{332} (c164) in our interface model and change of Asp^{332} (c164) to Tyr results in hemophilia B (see Haemophilia B data base).

Mutations in the hydrophobic patch of the interface model are also known to cause bleeding diathesis. Thus, mutation of Phe^{378} (c208) to Val or Leu in factor IXa causes hemophilia B (see Haemophilia B data base, available via the World Wide Web), and change of Ile^{566} to Thr or Arg in the A2 subunit causes hemophilia A (Ref. 12; see hemophilia data base, World Wide Web). The mutation of Ile^{566} to Arg is expected to disrupt the hydrophobic interaction. However, Thr substitution yields Asn-*X*-Thr consensus sequence that leads to a new *N*-glycosylation site at Asn^{564}, which could disrupt the Factor IXa:A2 subunit interaction. Moreover, change of Phe^{302} (c133) to Ala has been shown to impair the interaction of factor IXa with factor VIIIa (19). Mutations of Phe^{302} (c133) to Ala and Phe^{378} (c208) to Val or Leu are expected to diminish the hydrophobic interactions involving Ile^{566} and Met^{567} of the A2 subunit. The change of Ile^{566} to Arg in the A2 subunit would have similar consequences.

Concluding Remarks—Previous studies have indicated that the helix 330 (c162) of the protease domain (25) and 558–565 region of the A2 subunit (18) represent important determinants for the interaction of factor IXa and factor VIIIa, respectively. However, it was not known whether these two regions interact with each other in the IXa:VIIIa complex. The present study provides evidence that these two regions may form an interface and interact with each other involving hydrophobic as well as electrostatic forces (Fig. 6). Modeling of the interface suggests that other spatially nearby regions may also participate in the interaction of factor IXa with factor VIIIa. Several mutations in the proposed interface cause hemophilia A or B and are known to impair IXa:VIIIa interaction. Thus, our interface model is compatible with the existing biochemical as well as with the two-dimensional electron crystallography data of Stoylova *et al.* (20). However, the three-dimensional cocrystal structure of the factor IXa protease domain and A2 subunit will be required to fully establish this view. In light of these considerations, we emphasize that our interface model is an interim model subject to refinement as new biochemical and experimentally determined structural data become available.

Acknowledgments—We thank Tomasz Heyduk and Jim Kiefer for useful discussions. We also thank Lisa Regan and James Brown of Bayer Corp. and Debra Pittman of the Genetics Institute for providing the recombinant factor VIII, and Jennifer Chandler for excellent technical assistance.

REFERENCES

1. Mann, K. G. (1999) *Thromb. Haemostasis* **82,** 165–174
2. Bajaj, S. P., and Joist, J. H. (1999) *Semin. Thrombos. Hemostasis* **25,** 407–418
3. DiScipio, R. G., Kurachi, K., and Davie, E. W. (1978) *J. Clin. Invest.* **61,** 1528–1538
4. Brandstetter, H., Bauer, M., Huber, R., Lollar, P., and Bode, W. (1995) *Proc. Natl. Acad. Sci. U. S. A.* **92,** 9796–9800
5. Hopfner, K. P., Lang, A., Karcher, A., Sichler, K., Kopetzki, E., Brandstetter, H., Huber, R., Bode, W., and Engh, R. A. (1999) *Structure* **7,** 989–996
6. Bajaj, S. P., and Birktoft, J. J. (1993) *Methods Enzymol.* **222,** 96–128
7. Bajaj, S. P. (1999) *Thromb. Haemostasis* **82,** 218–225
8. Mertens, K., Celie, P. H. N., Kolkman, J. A., and Lenting, P. J. (1999) *Thromb. Haemostasis* **82,** 209–217
9. Vehar, G. A., Keyt, B., Eaton, D., Rodriguez, H., O'Brien, D. P., Rotblat, F., Opperman, H., Keck, R., Wood, W. I., Harkins, R. N., Tuddenham, E. G. D., Lawn, R. M., and Capon, D. J. (1984) *Nature* **312,** 337–342
10. Wood, W. I., Capon, D. J., Simonsen, C. C., Eaton, D. L., Gitschier, J., Keyt, B., Seeburg, P. H., Smith, D. H., Hollingshead, P., Wion, K. L., Delwart, E., Tuddenham, E. D. G., Vehar, G. A., and Lawn, R. M. (1984) *Nature* **312,** 330–337
11. Toole, J. J., Knopf, J. L., Wozney, J. M., Sultzman, L. A., Buecker, J. L., Pittman, D. D., Kaufman, R. J., Brown, E., Shoemaker, C., Orr, E. C., Amphlett, G. W., Foster, W. B., Coe, M. L., Knutson, G. J., Fass, D. N., and Hewick, R. M. (1984) *Nature* **312,** 342–347
12. Pemberton, S., Lindley, P., Zaitsev, V., Card, G., Tuddenham, E. G. D., and Kemball-Cook, G. (1997) *Blood* **89,** 2413–2421
13. Pratt, K. P., Shen, B. W., Takeshima, K., Davie, E. W., Fujikawa, K., and Stoddard, B. L. (1999) *Nature* **402,** 439–442
14. Lollar, P., and Parker, C. G. (1989) *Biochemistry* **28,** 666–674
15. Fay, P. J., Haidaris, P. J., and Smudzin, T. M. (1991) *J. Biol. Chem.* **266,** 8957–8962
16. Lollar, P., and Parker, G. G. (1990) *J. Biol. Chem.* **265,** 1688–1692
17. Fay, P. J., Smudzin, T. M., and Walker, F. J. (1991) *J. Biol. Chem.* **266,** 20139–20145
18. Fay, P. J., and Koshibui, K. (1998) *J. Biol. Chem.* **273,** 19049–19054
19. Kolkman, J. A., Lenting, P. J., and Mertens, K. (1999) *Biochem. J.* **339,** 217–221
20. Stoylova, S. S., Lenting, P. J., Kemball-Cook, G., and Holzenburg, A. (1999) *J. Biol. Chem.* **274,** 36573–36578
21. Freedman, S. J., Blostein, M. D., Baleja, J. D., Jacobs, M., Furie, B. C., and Furie, B. (1996) *J. Biol. Chem.* **272,** 22037–22045
22. Lenting, P. J., van de Loo, J.-W. H. P., Donath, M.-J. S. H., van Mourik, J. A., and Mertens, K. (1996) *J. Biol. Chem.* **271,** 1935–1940
23. Lapan, K. A., and Fay, P. J. (1997) *J. Biol. Chem.* **272,** 2082–2088
24. Fay, P. J., Beattie, T., Huggins, C. F., and Regan, L. M. (1994) *J. Biol. Chem.* **269,** 20522–20527
25. Mathur, A., and Bajaj, S. P. (1999) *J. Biol. Chem.* **274,** 18477–18486
26. Husten, E. J., Esmon, C. T., and Johnson, A. E. (1987) *J. Biol. Chem.* **262,** 12953–12966
27. Mimms, L. T., Zampighi, G., Nozaki, Y., Tanford, C., and Reynolds, J. A. (1981) *Biochemistry* **20,** 833–840
28. Bajaj, S. P., Rapaport, S. I., and Prodanos, C. (1981) *Prep. Biochem.* **11,** 397–412
29. Fay, P. J., Haidaris, P. J., and Huggins, C. F. (1993) *J. Biol. Chem.* **268,** 17861–17866
30. Curtis, J. E., Helgerson, S. L., Parker, E. T., and Lollar, P. (1994) *J. Biol. Chem.* **269,** 6246–6251
31. Bradford, M. M. (1976) *Anal. Biochem.* **72,** 248–254
32. Zhong, D., Smith, K. J., Birktoft, J. J., and Bajaj, S. P. (1994) *Proc. Natl. Acad. Sci. U. S. A.* **91,** 3574–3578
33. Zhong, D., and Bajaj, S. P. (1993) *BioTechniques* **15,** 874–878
34. Mathur, A., Zhong, D., Sabharwal, A. K., Smith, K. J., and Bajaj, S. P. (1997) *J. Biol. Chem.* **272,** 23418–23426
35. Halfman, C. J. (1981) *Methods Enzymol.* **74,** 481–408
36. Cheng, Y.-C., and Prusoff, W. H. (1973) *Biochem. Pharmacol.* **22,** 3099–3108
37. Craig, D. A. (1993) *Trends Pharmacol. Sci.* **14,** 89–91
38. Church, W. R., Jernigan, R. L., Toole, J., Hewick, R. M., Knopf, J., Knutson, G. J., Nesheim, M. E., Mann, K. G., and Fass, D. N. (1984) *Proc. Natl. Acad. Sci. U. S. A.* **81,** 6934–6937
39. Zaitseva, I., Zaitsev, V., Card, G., Moshkov, K., Bax, B., Ralph, A., and Lindley,

P. (1996) *J. Biol. Inorg. Chem.* **1,** 15–23
40. Peitsch, M. C. (1996) *Biochem. Soc. Trans.* **24,** 274–279
41. Guex, N., Diemand, A., and Peitsch, M. C. (1999) *Trends Biochem. Sci.* **24,** 364–367
42. Mann, K. G., Jenny, R. J., and Krishnaswamy, S. (1988) *Annu. Rev. Biochem.* **57,** 915–956
43. van Dieijen, G., Tans, G., Rosing, J., and Hemker, H. C. (1981) *J. Biol. Chem.* **256,** 3433–3442
44. Arni, R. K., Padmanabhan, K., Padmanabhan, K. P., Wu, T. P., and Tulinsky, A. (1994) *Chem. Phys. Lipids* **67/68,** 59–66
45. Laskowski, R. A., MacArthur, M. W., Moss, D. W., and Thornton, J. M. (1993) *J. Appl. Crystallogr.* **26,** 283–291
46. Nicholls, A., Sharp, K. A., and Honig, B. (1991) *Proteins* **11,** 281–296
47. Fay, P. J., and Scandella, D. (1999) *J. Biol. Chem.* **274,** 29826–29830
48. Lollar, P., Parker, E. T., Curtis, J. E., Helgerson, S. L., Hoyer, L. W., Scott, M. E., and Scandella, D. (1994) *J. Clin. Invest.* **93,** 2497–2504
49. Regan, L. M., Lamphear, B. J., Huggins, C. F., Walker, F. J., and Fay, P. J. (1994) *J. Biol. Chem.* **269,** 9445–9452